

UWB Propagation through Walls

Vladimír SCHEJBAL¹, Pavel BEZOUŠEK¹, Dušan ČERMÁK¹, Zdeněk NĚMEC¹, Ondřej FIŠER²,
Martin HÁJEK¹

¹ University of Pardubice, Studentská 95, 532 10 Pardubice, Czech Republic

² Institute of Atmospheric Physics, Boční Street II/1401, 141 31 Prague 4, Czech Republic

vladimir.schejbal@upce.cz, pavel.bezousek@upce.cz, dusan.cermak@upce.cz, zdenek.nemec@upce.cz,
ondrej@ufa.cas.cz, martin.hajek@upce.cz

Abstract. The propagation of ultra wide band (UWB) signals through walls is analyzed. For this propagation studies, it is necessary to consider not only propagation at a single frequency but in the whole band. The UWB radar output signal is formed by both transmitter and antenna. The effects of antenna receiving and transmitting responses for various antenna types (such as small and aperture antennas) are studied in the frequency as well as time domain. Moreover, UWB radar output signals can be substantially affected due to electromagnetic wave propagation through walls and multipath effects.

Keywords

Ultra wide band, UWB antennas, UWB propagation, multipath effects.

1. Introduction

UWB is defined by FCC as any radio technology having a spectrum that occupies a bandwidth greater than 20 percent of the center frequency, or a bandwidth of at least 500 MHz. The UWB concept is very useful for radars and communications, cf. [1] to [6]. A UWB engineer needs to be familiar with both the time domain and frequency domain, able to switch seamlessly from one domain to the other as the nature of problem demands.

UWB radar output signals are formed by both transmitter and antenna. Therefore the UWB antenna should be considered as an integral part of the whole system. A small antenna is here defined as an antenna occupying a small fraction of spherical volume having radius of one wavelength. The output transmitted signal should be usually formed by the UWB system requirements. That is why propagation analyses should be performed for very wide frequency spectrum and simultaneously, the effect of various transmitted signal shapes (e.g. pulses) should be analyzed as well as the effect of various antenna receiving and transmitting responses. Results for various combinations of signals, transmitting or receiving antennas (small and aperture antennas) and wall structures are calculated and

compared. Narrow band and ultra wide band (UWB) propagation is discussed in this contribution. The multipath effect is also considered. The propagation of electromagnetic waves through walls is analyzed for both frequency and time domains. The equations are derived for frequency domain and transformed using FFT into time domain. The technique, which allows the calculations of both frequency spectra and time responses for combinations of various antennas, input signals and several layers (walls), has been coded using the MATLAB® language. An example of calculations is shown in Fig. 1 for receiving aperture antenna.

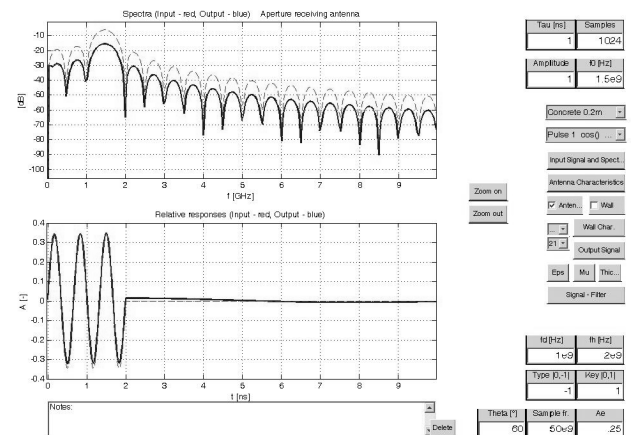


Fig. 1. An example of calculation of signal response in receiving aperture antenna in both frequency and time domain.

In many situations, harmonic functions offer a potentially misleading situation. For instance, any attempt to model an ideal step function using superposition of harmonic functions yields overshoot and ringing. Therefore, the utilization of Fourier transform (especially FFT, when aliasing can occur) should be analyzed very carefully. It is necessary to consider Gibbs phenomena (at points of discontinuity of signal, the error signal has a tendency to oscillate), sampling theorem (if a signal is sampled periodically at a rate $f_s = 1/T_s > 2B$, where B is the highest frequency contained in a continuous-time signal, the signal can be exactly recovered from the sample values) and simultaneously the number of sampling values N should be sufficient (for example the product $NT/2$ should be greater than time of

propagation through an analyzed distance as the discrete Fourier transform assumes that the finite duration time-series was periodically extended in all time). The Gibbs phenomenon cannot be present for a signal, which is piecewise continuous with its first derivative at the point, where a signal is continuous.

2. Signal Transmission and Reception

Antenna transmitting and receiving responses for various UWB antenna types (such as small and aperture antennas) should be considered as they are not exactly the same. It was shown both theoretically and experimentally that the transmitting transient response of an antenna is proportional to the time derivative of the receiving transient response of the same antenna (e.g. [3] and [7]). That can be derived applying the Rayleigh-Carson reciprocity theorem or a plane-wave scattering theory [7]. Alternatively, that can be demonstrated analyzing signal reception, when the Poynting vector and the effective area A_e should be considered and signal transmission, when gain G and transmitted power should be used. Using the well known equation [8]

$$G = \frac{4\pi}{\lambda^2} A_e = \frac{4\pi^2 f^2}{\pi c^2} A_e = \frac{\omega^2}{\pi c^2} A_e \quad (1)$$

where λ is the wavelength, f is the frequency, c is the speed of light in vacuum and $\omega = 2\pi f$, it is clear that an extra $j\omega$ factor exists in the relation between transmitted and received fields as the relation (1) is derived using transmitted and received power. That was ignored in the classical frequency domain antenna design and everyone has assumed that an antenna's gain is identical for either transmitting or receiving. For engineers working in the frequency domain at a single frequency, or a narrow band of frequencies, this $j\omega$ term simply amounts to a 90-degree phase shift term, i.e. converts the frequency domain sine wave into a cosine wave. In the time domain, however, this $j\omega$ term has a dramatically different effect of either differentiating or integrating, depending upon the usage of an antenna. The stationary phase method for plane aperture antennas gives for aperture at the xy plane (details can be found in [8])

$$\begin{aligned} \mathbf{E}(\mathbf{r}) &\approx \frac{j\omega \cos\theta}{2\pi r} \exp[j\omega(t - r/c)] \\ &\times \iint_S \mathbf{E}_t(x, y, 0) \exp(jk_x x + jk_y y) dx dy \end{aligned} \quad (2)$$

where \mathbf{E}_t is the aperture electric field and k_x, k_y are components of propagation vector \mathbf{k} and r is the distance. That shows that the plane-aperture antenna response is given by differentiating due to the $j\omega$ term. For small antennas, the gain is nearly constant and therefore the response is not changed. Therefore, aperture antennas are analyzed using (2) considering the fact that they should be considered as small antennas for lower frequencies. Stating the exact border between small and aperture antennas is not possible. Thus the limit was chosen rather arbitrarily considering the

asymptotic behavior of these antennas. The gain of aperture antennas is given by (1), while the gain of small antennas $G \approx 1$. Therefore the limit is chosen using (1) for $G = 1$ considering the effective area $A_e = A \varepsilon_T$, where A is the aperture area and ε_T is the aperture (taper) efficiency (A_e can be roughly considered as a constant). The rough estimation for ε_T is 0.8 (usually 0.5 to 1 - see examples in [9]).

On the other hand the receiving antenna response will be integrated due to the term $1/(j\omega)$ for small antennas according to (1) and the response will not change in the case of plane aperture antennas. Naturally, the same limit between small and aperture antennas has been chosen.

Of course, the real antennas cannot work from DC to infinity and therefore, they form a band-pass filter. Hence, the real antennas do not exactly perform differentiation or integration, their responses are causal and relative input and output spectra and responses could only be considered (theoretically, the well-known Parseval's theorem should be considered for the absolute spectra calculation and that cannot be done without knowledge of particular antenna spectra). It is clear that relative spectra and responses could be rather confusing.

3. Antenna Input and Output Signals

In this section, various input signals are analyzed. It was observed that transmitting small antenna and receiving aperture antenna (for higher frequencies) do not distort the input signal, and therefore those are not shown here (except receiving aperture antenna, which is given as an example in Fig. 1). Rectangular pulses with various rise and fall times and the following special shaped pulses have been analyzed

$$s_n(t) = a_n(t) \cos \omega_0 t \quad (3)$$

where $\omega_0 = 2\pi f_0$ and f_0 is the frequency. The following pulse types have been chosen for $a(t)$ function (transmitted signal is formed according to the UWB system requirements).

Pulse 1

$$\begin{aligned} a_1(t) &= 1 \quad \text{for } t \in \langle -\tau_0, +\tau_0 \rangle \\ &= 0 \quad \text{for } t \notin \langle -\tau_0, +\tau_0 \rangle \end{aligned}$$

Pulse 2

$$\begin{aligned} a_2(t) &= 1 - \left| \frac{t}{2\tau_0} \right| \quad \text{for } t \in \langle -2\tau_0, +2\tau_0 \rangle \\ &= 0 \quad \text{for } t \notin \langle -2\tau_0, +2\tau_0 \rangle \end{aligned}$$

Pulse 3

$$\begin{aligned} a_3(t) &= \cos^2 \left(\frac{\pi t}{4 \tau_0} \right) \quad \text{for } t \in \langle -2\tau_0, +2\tau_0 \rangle \\ &= 0 \quad \text{for } t \notin \langle -2\tau_0, +2\tau_0 \rangle \end{aligned}$$

Considering various antenna receiving and transmitting responses and various input signals many various combinations have been calculated and compared using the above described code. It is not possible to show all numerical simulations. Therefore some of calculated spectra are only given for pulses with $\tau_0 = 1$ ns, $\omega_0 = 2\pi f_0$ and $f_0 = 1.5$ GHz in Figs. 2 to 4 for aperture transmitting antenna and small receiving antenna as small transmitting antenna and aperture receiving antenna (see Fig. 1) practically do not change the spectra. Many other examples (with $f_0 = 4$ GHz and $\tau_0 = 0.5$ ns) can be found in [10].

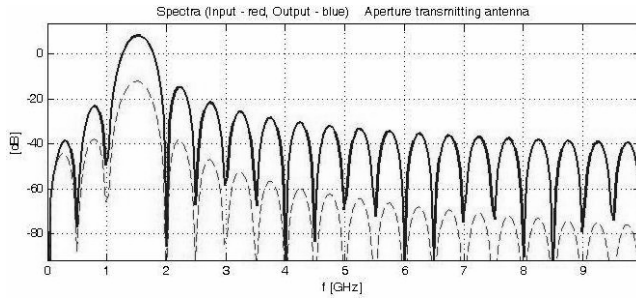


Fig. 2. Relative input and output (solid line) spectra for transmitting aperture antenna (pulse 2 with $\tau_0=1$ ns and $f_0 = 1.5$ GHz).

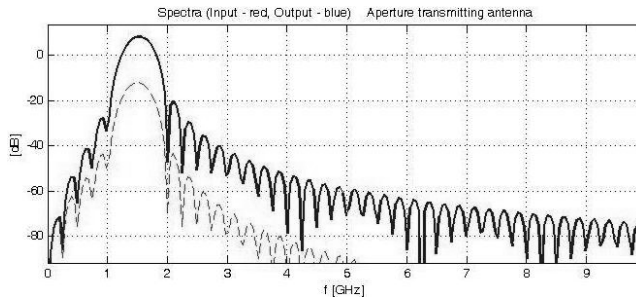


Fig. 3. Relative input and output (solid line) spectra for transmitting aperture antenna (pulse 3 with $\tau_0=1$ ns and $f_0 = 1.5$ GHz)

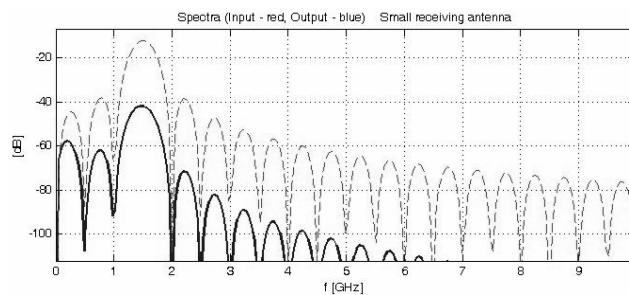


Fig. 4. Relative input and output (solid line) spectra for small receiving antenna (pulse 2 with $\tau_0 = 1$ ns and $f_0 = 1.5$ GHz)

4. Propagation through Walls

Analyses can be done considering oblique incidence of plane waves at dielectric layers (walls) and propagation through particular layers [11]. A plane wave obliquely

incident at the angle θ_1 from the normal to the plane boundary between two dielectric regions can be calculated using the wave impedance Z in the plane of incidence (TM waves) and normal to that plane (TE waves)

$$Z_{z1TM} = \frac{E_{x+}}{H_{y+}} = -\frac{E_{x-}}{H_{y-}} = \sqrt{\mu_1/\epsilon_1} \cos \theta_1, \quad (4)$$

$$Z_{z1TE} = \frac{E_{y+}}{H_{x+}} = -\frac{E_{y-}}{H_{x-}} = \frac{\sqrt{\mu_1/\epsilon_1}}{\cos \theta_1}, \quad (5)$$

where E and H are electric and magnetic fields propagating in the forward (+) or backward direction (-), ϵ_1 and μ_1 are permittivity and permeability of layer 1, respectively.

Snell's law says (θ_1 is an incident angle and θ_2 is a reflected angle)

$$k_1 \sin \theta_1 = k_2 \sin \theta_2, \quad (6)$$

where $k_m = \omega \sqrt{(\epsilon_m \mu_m)}$, $\omega = 2\pi f$.

Coefficients of reflection ρ and transmission τ are given by [11]

$$\rho = \frac{E_{1-}}{E_{1+}} = \frac{Z_{z2} - Z_{z1}}{Z_{z2} + Z_{z1}}, \quad \tau = \frac{E_2}{E_+} = \frac{2Z_{z2}}{Z_{z2} + Z_{z1}}, \quad (7)$$

where (4) or (5) should be used for TM or TE waves.

That allows the calculation of the UWB propagation through walls using $[S]$ scattering matrix of boundaries $[S]_I$ and layers $[S]_P$ (subscript P is used for plane wave). For individual boundaries and layers with thickness t_m , the following equations are valid

$$[S]_I = \begin{bmatrix} \frac{Z_{z2} - Z_{z1}}{Z_{z2} + Z_{z1}} & \frac{2Z_{z1}}{Z_{z2} + Z_{z1}} \\ \frac{2Z_{z2}}{Z_{z2} + Z_{z1}} & \frac{Z_{z1} - Z_{z2}}{Z_{z2} + Z_{z1}} \end{bmatrix}, \quad (8)$$

$$[S]_P = \begin{bmatrix} 0 & e^{-jt_m k_m \cos \theta_m} \\ e^{-jt_m k_m \cos \theta_m} & 0 \end{bmatrix}. \quad (9)$$

Then scattering matrices can be changed into transmission matrices $[T]$, which can be used for calculation of cascade connecting two-ports. This model (plane wave) could be used for greater distances between antenna and wall.

Because the smaller distances are typical for UWB communication and radars, the spherical waves (geometrical optics) should be considered. Then a different matrix $[S]_S$ should be used [12]

$$[S]_S = \begin{bmatrix} 0 & D_m e^{-jt_m k_m / \cos \theta_m} \\ D_m e^{-jt_m k_m / \cos \theta_m} & 0 \end{bmatrix} \quad (10)$$

where D_m is a divergence factor

$$D_m = \sqrt{\frac{r_1 r_2}{(r_1 + l)(r_2 + l)}} \quad (11)$$

where r_1 and r_2 are principal radii of wave-front and l is a distance between a wave-front and observation point on the other wave-front. For a spherical wave, $r_1 = r_2 = r$ and therefore $D_m = r / (r + l)$, for cylindrical wave $r_1 \rightarrow \infty$, or possibly $r_2 \rightarrow \infty$ and $D_m = r_2 / (r_2 + l)^{1/2}$ and finally for a plane wave $r_1 \rightarrow \infty$ and $r_2 \rightarrow \infty$, so $D_m = 1$ (no spreading).

It can be noticed that phases in $[S]_P$ and $[S]_S$ are substantially different due to the fact that plane or spherical wave-fronts should be considered for phase calculations.

The parameters s_{11} and s_{21} for various walls have been calculated. Some of them (for a wave having incident angle $\theta_1 = 0$) are shown in Figs. 5 to 9.

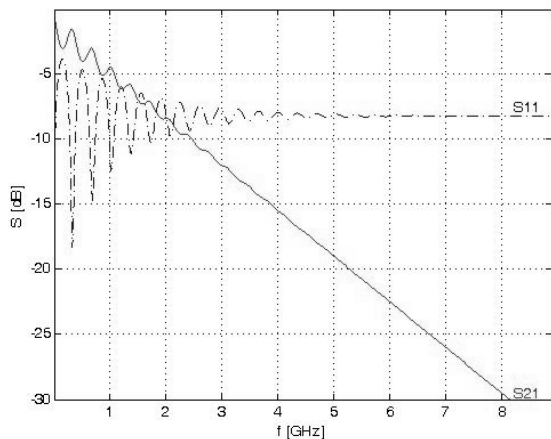


Fig. 5. Parameters s_{11} and s_{21} for wall 1.

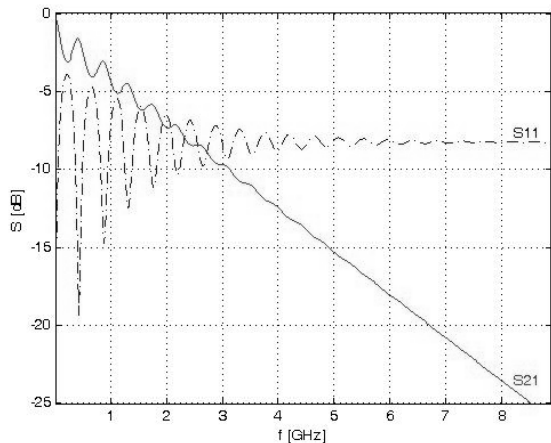


Fig. 6. Parameters s_{11} and s_{21} for wall 2.

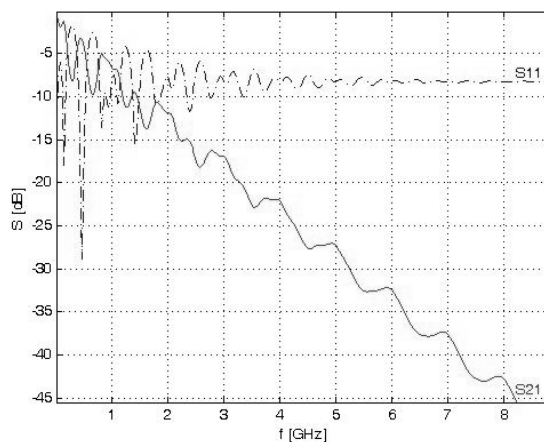


Fig. 7. Parameters s_{11} and s_{21} for wall 3.

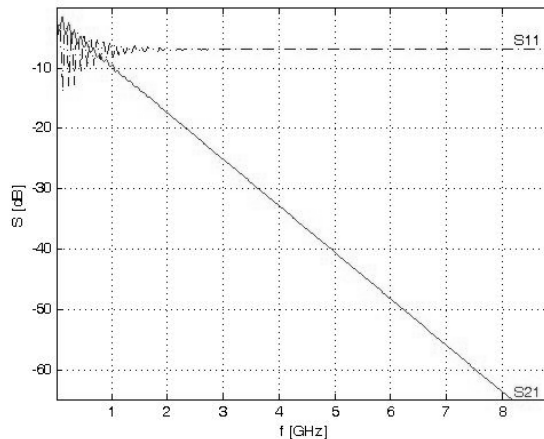


Fig. 8. Parameters s_{11} and s_{21} for wall 4.

Wall No.	Type	ϵ'	ϵ''	Thickness t [m]
1	Brick wall	5.1	0.46	0.19
2	Brick wall	5.1	0.46	0.15
3	Brick wall	5.1	0.46	0.28
4	Concrete wall	7	0.45	0.5
5	Concrete wall	7	0.45	0.15

Tab. 1. Electrical parameters of walls.

The described method assumes that ϵ and μ can be frequency-dependent but the used code supposes those parameters to be constant for any layer. Certainly, the code could be easily changed allowing to enter frequency changes of ϵ and μ . The assumption that ϵ and μ are roughly constant has been used, because published experimental wall electrical properties (e.g. [13] and [14]) have been thoroughly analyzed and numerical simulations have been extensively compared with both published theoretical (for plane as well as spherical waves) and experimental results. It can be concluded that the used assumption could be successfully accepted. The chosen wall parameters are given in Tab. 1, where relative permittivities $\epsilon_r = \epsilon' - j\epsilon''$ with various wall thicknesses t are given for both brick (wall 1, 2 and 3) and concrete walls (wall 4 and 5). Relative permeability $\mu_r = 1$ is supposed.

5. Time Domain Analysis

Lack of information cannot be replaced by any mathematical operation and therefore new information cannot be obtained using Fourier transform. That means that complex spectra contain any relevant information. The output signal spectra are certainly very important for vari-

ous purposes such as EMC analyses but they cannot show various phenomena such as shapes and delays. Therefore, it is much more convenient to use inverse Fourier transform (IFFT) and analyze the signal responses in the time domain. Various antenna receiving and transmitting responses and various input signals and walls have been analyzed. Some of them are only shown in Fig. 10 to 18. Many others can be found in [10].

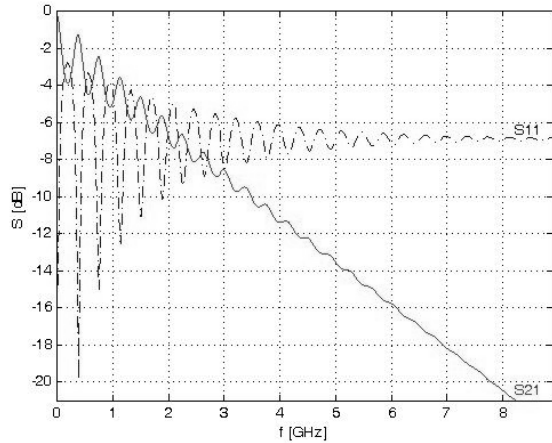


Fig. 9. Parameters s_{11} and s_{21} for wall 5.

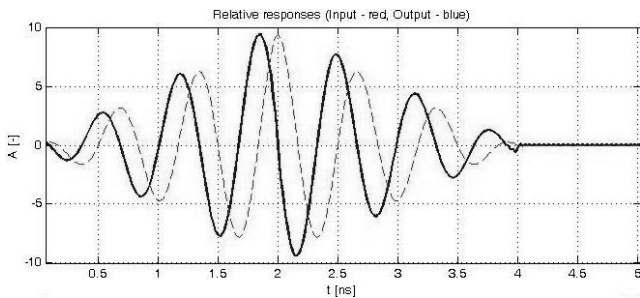


Fig. 10. Relative input and output (solid line) signals for aperture transmitting antenna and pulse 2 with $\tau_0 = 1$ ns and $f_0 = 1.5$ GHz – antenna output delay is not included.

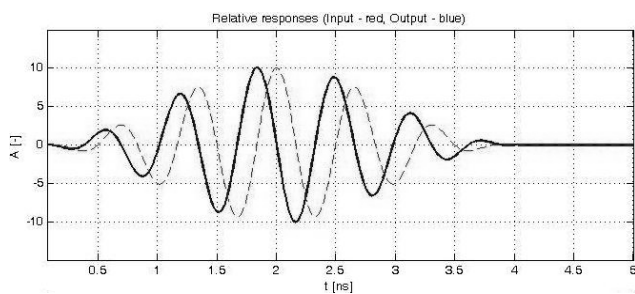


Fig. 11. Relative input and output (solid line) signals for aperture transmitting antenna and pulse 3 with $\tau_0 = 1$ ns and $f_0 = 1.5$ GHz – antenna output delay is not included.

Antenna receiving and transmitting responses as well as UWB signals (pulses) are analyzed above from the spectrum point of view (cf. also [10]). Therefore responses, i.e. input and output signals, calculated using inverse Fourier transform (IFFT) for several pulses are plotted in Figs. 10 to 12 for aperture transmitting antenna and small receiving antenna. Small transmitting antenna and aperture receiving antenna do not practically change the spectra and therefore

they are not shown. The antenna output delays are not included as they depend on the propagations along transmission lines and the properties of particular antennas. The effect of the used antenna can be seen (differentiation for Figs. 10 and 11 and integration for Fig. 12). That would be fulfilled for ideal antennas. The real antennas form a band-pass filter and therefore do not exactly perform differentiation or integration and their responses are causal.

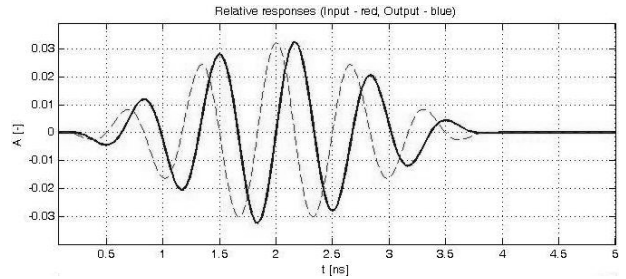


Fig. 12. Input and output (solid line) signals for small receiving antenna and pulse 3 with $\tau_0 = 1$ ns and $f_0 = 1.5$ GHz – antenna output delay is not included.

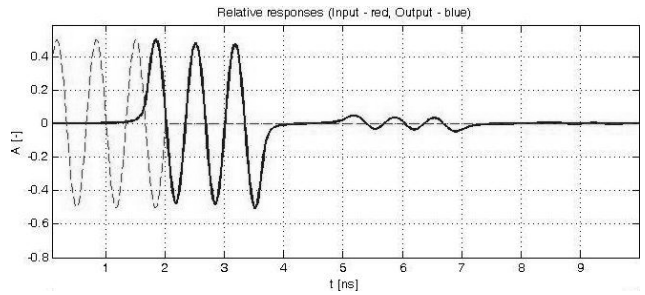


Fig. 13. Relative input and output (solid line) signals (pulse 1) for small transmitting antenna and propagation through brick wall 1 (thickness $t = 0.19$ m).

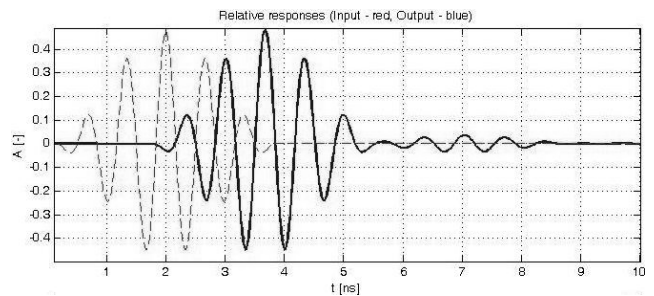


Fig. 14. Relative input and output (solid line) signals (pulse 3) for small transmitting antenna and propagation through brick wall 1 ($t = 0.19$ m).

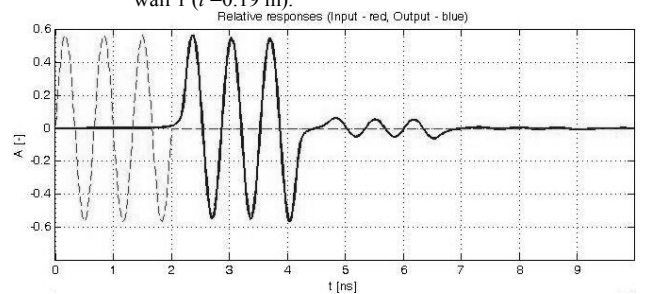


Fig. 15. Relative input and output signals (pulse 1) for small transmitting antenna and propagation through brick wall 3 ($t = 0.28$ m).

If the parameter s_{21} is known (calculated), it is possible to obtain the output signal spectrum $b_2(\theta_0)$ for any point (θ_0 is incident angle) both for TE and TM waves

$$b_2(\theta_0) = s_{21}(\theta_0)a_1(\theta_0) \quad (12)$$

where $a_1(\theta_0)$ is the input signal spectrum. It is much more convenient to use inverse Fourier transform (IFFT) and analyze the signal responses in the time domain. Several cases of propagation through walls have been analyzed. Some of them are shown in Figs. 13 to 18.

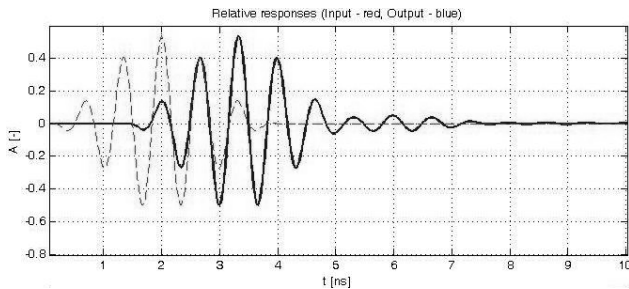


Fig. 16. Relative input and output signals (pulse 3) for small transmitting antenna and propagation through brick wall 3 (0.28 m thickness).

The delay and ringing (due to multiple reflections at boundaries) can be clearly seen. Naturally, the interferences (disturbing) of multiple reflections are much smaller for very short pulses in comparison with the CW and narrow-band applications.

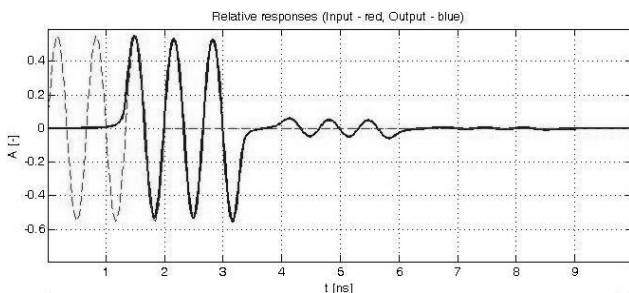


Fig. 17. Relative input and output signals for (pulse 1) for small transmitting antenna and propagation through concrete wall 5 (0.15 m thickness).

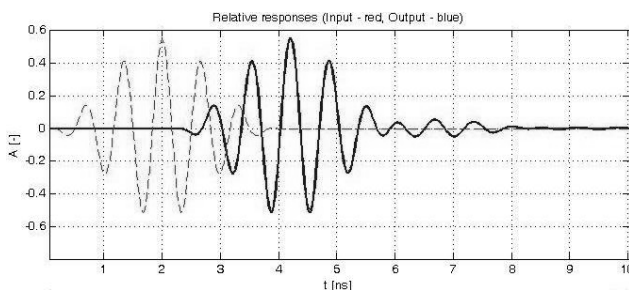


Fig. 18. Relative input and output signals for (pulse 3) for small transmitting antenna and propagation through concrete wall 5 (0.15 m thickness).

Determination of propagation of plane waves through several layers is a standard method [11]. Utilization of spherical waves (i.e. geometrical optics) is not quite usual. However, the geometrical optics offers very simple and

fast methods for numerical simulations in comparison with various numerical methods (such as MoM) or physical optics. Moreover, it has been shown that the accuracy of geometrical optics is fully acceptable.

6. Multipath Effects

The multipath effects should be considered for the UWB systems. The most common case is given in Fig. 19 where direct and reflected signals are shown. Usually, it is not possible to consider one reflection only but the other reflections should be taken into account due to a ground, walls and nearby objects. Both direct and reflected signals propagate through wall and they can be calculated directly (see previous parts).

The spectrum of reflected signal is modified (multiplied) by the reflection coefficient of ground (or possibly of another object)

$$b_{2r}(\theta_r) = S_{21}(\theta_r)a_1(\theta_r)\rho_s(\alpha), \quad (13)$$

where $\rho_s(\alpha)$ is the reflection coefficient at the given surface, which can be calculated as a reflection from a dielectric layer. Of course, surface properties at the related angle α should be considered. The other parameters are the same like in equation (13) but the different angle θ_r should be considered.

The reflection coefficient can be obtained by the above described technique, too. As it has been stated it is much more convenient to analyze the signal responses in the time domain using inverse Fourier transform (IFFT).

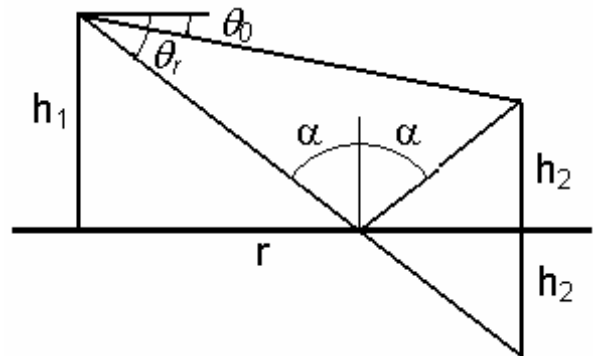


Fig. 19. Direct and reflected rays.

Various cases have been simulated numerically. Direct and reflected signals for small transmitting antenna and propagation through wall 5 and pulse 1 are shown in Fig. 20 for TE waves. The ground with $\epsilon_r = 7 - j0.45$ and $t = 0.15$ m, heights $h_1 = 1.5$ m and $h_2 = 0.4$ m and distance $r = 3$ m were considered.

Various delays (due to propagation through wall along various paths of direct and reflected rays) and the ringing (similar to UWB propagation through wall) can be clearly seen. Certainly, these phenomena are much more pronounced for reflected rays. On the other hand, the inter-

ference effects of multiple reflections and multipath effects are much smaller for UWB signals than for CW narrow-band applications as interference minima and maxima do not occur for the same frequencies. Moreover for very short pulses, the individual pulses are received at various times and can be distinguished more easily.

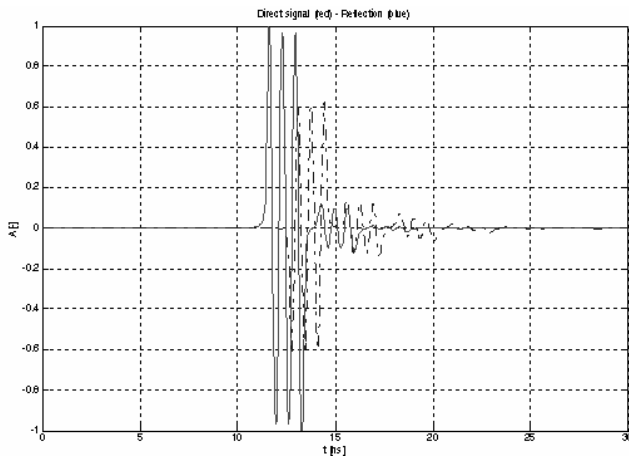


Fig. 20. Direct (solid line) and reflected signals for small transmitting antenna, heights $h_1 = 1.5\text{ m}$ and $h_2 = 0.4\text{ m}$, distance $r = 3\text{ m}$, wall 5 and pulse 1.

A similar approximate model was developed for the propagation of a spherical electromagnetic wave through a building wall of known material properties in [15], which is shown to be in a good agreement with measured results. That model is based on the method of images and geometrical optics and in contrast to the above method uses an equivalent source approach, when the original source is replaced by an equivalent source (that operation is not straightforward and uses total received field, which it is found by integrating over the aperture). Then the wall is removed and the equivalent source radiates in free space. Multiple reflections inside of the wall are neglected in that model. It is said that the equivalent source method could be expanded to include multiple reflections by introducing an additional equivalent source for each multiple reflection added but that seems to be very complicated (the above described method computes multiple reflections inside of the walls automatically, as that has been demonstrated in Fig. 13 to 18 and 20).

7. Conclusions

The described methods have been coded using the MATLAB® language. That allows numerical simulations for both frequency spectra and time responses for many combinations of various antennas, input signals, several layers (walls) and multipath effects. As far as the authors know, similar extensive numerical simulations have not been published (especially for UWB time responses).

Various combinations of UWB antenna types (such as small and aperture antennas) for receiving and transmitting antennas and input signals have been calculated and com-

pared. Some of them can be only shown with $f_0 = 1.5\text{ GHz}$, $\tau_0 = 1\text{ ns}$. It can be concluded that the UWB radar-output transmitted signals are formed by both transmitters and antennas. The transmitting transient response of an ideal antenna is proportional to the time derivative of the receiving transient response of the same antenna. Therefore, UWB antennas should be considered as an integral part of the whole systems. Moreover, the output transmitted signal should be formed according to UWB system demands. That means that analyses should be done for very wide frequency spectrum and simultaneously, the effect of input signals (e.g. special shaped pulses) should be considered for both transmitting and receiving antennas.

The real antennas cannot work from DC to infinity and therefore, they form band-pass filter. Hence, the real antennas do not exactly perform differentiation or integration. However, it can be seen comparing the above given numerical simulations with published experimental results (such as [3] and [6]) that the above used antenna approximations can be successfully used for both frequency spectra and time responses.

The propagation of electromagnetic waves through a wall obstacle has been analyzed. The wall parameters are given for both brick and concrete walls with various thicknesses, where s_{11} and s_{21} can be found for these cases (cf. Figs 5 to 9). Preliminary experimental results are published in [10]. The described method has been extensively compared with both published theoretical and experimental results for frequency domain. It can be concluded that the described method could be successfully used.

The output signal spectra are certainly very important for various purposes such as EMC analyses but they cannot show various phenomena such as shapes and delays. The responses (input and output signals calculated using the IFFT) were extensively analyzed. Some of them are only shown in Figs. 10 to 18. The ringing (due to boundary multiple reflections) can be clearly seen. Naturally, the interference (disturbing) of multiple reflections is much smaller for very short pulses than for CW and narrow-band applications. The published results relevant to comparison with numerical simulations of time responses have not been available.

The described method can be easily used for analyses of multipath propagation due to reflections (such as ground or wall reflections). An example (Fig. 20) shows delays (due to propagation through wall and various paths of direct and reflected rays) and the ringing (similar to UWB propagation through wall). Certainly, these phenomena are much more pronounced for reflected rays. On the other hand, the interference effects of multiple reflections and multipath effects are much smaller for UWB signals than for CW narrow-band applications as interference minima and maxima do not occur for the same frequencies. Moreover for very short pulses, the individual pulses are received at various times and can be distinguished more easily. The published results relevant to comparison with numerical simulations of time responses have not been

available. However, many experiments concerning multipath time responses have been published and generally derived conclusions using experiments, field measurements and various analyses (including statistical approaches) agree with the above described numerical simulations (e.g. cf. [1], [2]).

Acknowledgements

This work has been supported by the grant of UWB Technology for Radars FT-TA2/030. The project has been realized using financial support of state budget assets by the Ministry of Industry and Trade.

We thank anonymous peer referees for drawing our attention to a correction of some sentences and improving of the paper.

References

- [1] HEYMAN, E., MANDELBAUM, B., SHILOH, J. *Ultra-Wideband Short-Pulse Electromagnetics* 4. New York: Plenum Press, 1999.
- [2] TAYLOR, J. D. *Ultra-Wideband Radar Technology*. N. York: CRC, 2001.
- [3] ANDREWS, J. R. UWB Signal sources, antennas & propagation. *Application Note AN -14a*. Picosecond Pulse Labs, Boulder, USA. August, 2003.
- [4] BEZOUŠEK, P., SCHEJBAL, V. Radar technology in the Czech Republic. *IEEE Aerospace & Electronic Systems Magazine*, 2004, vol. 19, no. 8, p. 27 - 34.
- [5] JOHNK, R.T et al. Time-domain measurements of radiated a conducted UWB Emissions. *IEEE Aerospace & Electronic Systems Magazine*, 2004, vol. 19, no. 8, p. 18 - 26.
- [6] SCHANTZ, H. *The Art and Science of Ultrawideband Antennas*. Boston, Artech House, 2005.
- [7] MILLER, E. K. *Time-Domain Measurements in Electromagnetics*. New York: Van Nostrand Reinhold, 1986.
- [8] COLLIN, R. E. *Antennas and Radiowave Propagation*. N. York: McGraw-Hill, 1985.
- [9] SCHEJBAL, V. Directivity of planar antennas. *IEEE Antennas and Propagation Magazine*, 1999, vol. 41, no. 2, p. 60 - 62.
- [10] SCHEJBAL, V. et al. UWB radar signal propagation through walls and multipath effects. *IEEE Aerospace & Electronic Systems Magazine*. Submitted to publication.
- [11] RAMO, S., WHINNERY, J. R., VAN DUZER, T. *Fields and Waves in Communication Electronics*. N. York: J. Wiley & Sons, 1994.
- [12] BHATTACHARYYA, A. K. *High-Frequency Electromagnetic Techniques: Recent Advances and Applications*. N. York: J. Wiley & Sons, 1995.
- [13] PEŇA, D., FEICK, R., HRISTOV, H. D., GROTE, W. Measurement and modeling of propagation losses in brick and concrete walls for the 900-MHz band. *IEEE Transactions on Antennas and Propagation*, 2003, vol. 51, no. 1, p. 31 - 39.
- [14] SOUTSOS, M. N., BUNGEY, J. H., MILLARD, S. G., SHAW, M. R., PATTERSON, A. Dielectric properties of concrete and their influence on radar testing. *NDT&E International*, 2001, vol. 34, p. 419 - 425.
- [15] GIBSON, T. B., JENN, D. C. Prediction and measurement of wall insertion loss. *IEEE Transactions on Antennas and Propagation*, 1999, vol. 47, no. 1, p. 55 - 57.

About Authors...

Vladimír SCHEJBAL was born in 1941. He received his M. Sc. from the Czech Technical University in Prague in 1970 and his PhD from the Slovak Academy of Sciences in Bratislava in 1980. He was with the Radio Research Institute of Tesla Pardubice from 1969 till 1993. He has been with the University of Pardubice since 1994. He is interested in numerical methods, simulations, measurements, radar antennas and propagation.

Pavel BEZOUŠEK was born in Ostrava, Czechoslovakia in 1943. He received his M. Sc. degree from the Czech Technical University in Prague in 1966 and his PhD degree from the same university in 1980. He was with the Radio Research Institute of the Tesla Pardubice from 1966 till 1994, where he was engaged in microwave circuits and systems design. Since then he is with the University of Pardubice, now at the Institute of Electrical Engineering and Informatics. Presently he is engaged in radar systems design.

Dušan ČERMÁK was born in 1974. He received his M.Sc. from the Czech Technical University in Prague in 2003. He has been with the University of Pardubice since 2003. He is interested in propagation of electromagnetic waves.

Zdeněk NĚMEC was born in 1977. He received Master degree in Electric transport equipment at the Jan Perner Transport Faculty, University of Pardubice in 2000. He has been with the University of Pardubice since 2002. He is interested in signal and data processing.

Ondřej FIŠER was born in Prague, 1952. He received the Ing. (M.Sc.) degree (1977) in electrical engineering and his CSc. (Ph.D.) degree (1986) in electronics, both from the Czech Technical University in Prague. He works as a scientific researcher at the Institute of Atmospheric Physics of the Czech Academy of Sciences focusing on radiowave propagation through the atmosphere and radar meteorology. He also teaches the electrical engineering at the University of Pardubice.

Martin HÁJEK was born in 1978. In 2001 he graduated (MSc.) at the Department of Electric, Electronic and Signaling in Transport of the Jan Perner Transport Faculty of University of Pardubice. Since 2001 he is Ph.D. student. His scientific research is focusing on FMCW radars and digital signal processing.